Vietnam Journal of Catalysis and Adsorption
Tạp chí xúc tác và hấp phụ Việt Nam

http://chemeng.hust.edu.vn/jca/

Electroactivity and electrochemical stability of Graphene-PANI nanocomposites for supercapacitor electrodes

Quang Minh Nguyen*, Minh Dang Nguyen, Lien Thi Tran, Thao Thi Nguyen, Thu Ha Thi Vu

Key Laboratory for Petrochemical and Refinery Technologies, 2 Pham Ngu Lao street, Hanoi, Vietnam

**Email: nguyenminhbk1502@gmail.com*

ARTICLE INFO

Received: 9/11/2018
Accepted: 11/12/2018

Keywords:
Graphene, PANI, Specific capacitance, Coulombic efficiency.

ABSTRACT

In this paper, a nanocomposite of reduced graphene oxide and polyaniline (rGO/PANI) was prepared by in-situ method, which can be directly used as electrodes materials for a flexible supercapacitor. That rGO was dispersed on PANI supporter created a rGO/PANI nanocomposite which has high surface area. At the same current density, the specific capacitance of rGO/PANI is 1121.2 F g^{-1}, while that of rGO is 182.7 F g^{-1} at 1 A g^{-1} in H_2SO_4 1 M medium. After 3000 cycles working at 5 A g^{-1}, the specific capacitance retention of rGO/PANI is about 75 % compared to the first cycle, higher than rGO (62.7 %). The graphene and conductive polymer combination, which formed a high electroacitvity and electrochemical stability nanocomposite, can be applied on coating material of supercapacitor electrode.

Introduction

Supercapacitor is a device that is capable of fast charging and discharging, which has much higher energy storage than conventional capacitors. To meet the advanced technical requirements in manufacturing supercapacitors, the spongy materials with high surface area were usually used to coat on the electrode surface. Among those materials, owing to its high specific surface area and excellent conductivity, graphene has been drawing tremendous attention.

The specific capacitance values of the supercapacitors with electrodes coated by graphene-based materials, published in the studies, range from 100 to nearly 2000 F g^{-1} [1-5]. In general, there are two ways to use graphene in electrode fabrication of supercapacitor: first, graphene material as electrode for dual-layer electrostatic deposition supercapacitor [1, 2]; second, graphene as a part of combination with metal oxides [3, 4] or conductive polymers used as electrode for fake electrochemical capacitor supercapacitors [5, 6].

For the first approach, graphene oxide is mainly used as an intermediate. However, the conductivity of the reduced graphene oxide needs to be improved and the number of layers of graphene should be reduced in order to increase the specific surface area. In the second approach, the graphene material combined with metal oxides, such as MnO_2 [7, 8] and RuO_2 [9, 10], or the graphene-polymers complexes, which have high specific capacitance values, improves the conductivity of the graphene, and at the same time results in the combination of graphite-based dual-layer electrostatic deposition and redox reaction. Whereas graphene-metal oxide composite material should be studied to improve the ability to disperse metal oxide on the surface of graphene and develop the overall

surface area of the graphene-polymer material, the graphene-polymer material system not only owns a large surface area, but also enhances the durability of the material during charging and discharging when supercapacitor is working.

This paper presents the results of the investigations of the electroactivity of graphene-PANI as well as the stability during the charge-discharge of this material in electroplating applications of supercapacitor.

Experimental

All chemicals were purchased from Sigma Aldrich. Deionized water was used throughout the study. Graphene oxide (GO) was synthesized by the modified Hummers method as presented in [11]. For the synthesis of reduced graphene oxide (rGO), GO was dispersed in ethylene glycol (EG) solution and stirred at 120 °C for 24 h. Afterwards, PANI was added to solution of 1.5 g rGO in 100 mL HCl 0,5 M, with ratio m_{PANI}/m_{rGO} = ½, the mixture was stored at 5 °C. Then, 1.25 g ammoni pesulfat (pre-cooled 5 °C) was poured into the above mixture, and the resultant mixture was left at 5 °C for 5 h. The obtained nanocomposite foam was filtered, washed untill pH = 7. Then it was dispersed in a mixture containing 0,9 mL deionized water and 0,3 mL Nafion 1 % under ultrasonication for 30 min.

Powder XRD patterns of samples were recorded with a D8 Advance diffractometer (Bruker). The morphology and microstructure of samples were investigated with a transmission electron microscope (TEM) JEOL JEM 2010 equipped operated at 200 kV. Surface area and pore size distribution of the samples were obtained by the BET measurement in the ASAP 2010 nitrogen adsorption equipment. Electrochemical measurements were performed on a CPA-ioc-HH5B Polarographic Analyser with a conventional three-electrodes cell. The working electrode is a glassy carbon electrode (5 mm in diameter), which was coated with 10 µL of the above catalyst ink and dried at room temperature. The counter electrode is a platinum electrode and the reference electrode is an Ag/AgCl. The electrochemical solution (H_2SO_4 1M) was deaerated by pure nitrogen gas prior to measurements.

The electrochemical operability of the material was evaluated by the specific capacitance (C_s) [4, 10], using the following equation:

$$C_s = \frac{dQ}{dV} = \frac{idt}{dV} = \frac{i}{\sqrt{}} \quad (1)$$

Where, C_s is the specific capacitance (F g^{-1}), Q is the charge stored by each electrode (C g^{-1}), V is the potential (V), i is the current density (A g^{-1}) - calculated from CV curves, √ is the potential scan rate (V s^{-1}). The CV analysis was carried at various scan rates, ranging from 1 to 100 mV s^{-1}, in a potential range of 0 ÷ 1 V.

$$C_s = \frac{I\Delta t}{m\Delta V} \quad (2)$$

Where, m is the mass of electroactive material (g), I is the current applied (A), Δt is the discharging time (s), ΔV is the potential range (V). All these values were identified by the gavanostatic charge/discharge techniques in H_2SO_4 1 M solution, in a potential range of 0 ÷ 1 V, at different current density 1, 2, 3, 4, 5 mA mg^{-1}.

The Coulombic efficiency of material was calculated using the following equation [12]:

$$\eta = (t_D*100)/t_C \ (\%) \quad (3)$$

Where, η is the Coulombic efficiency of material (%), t_D and t_C are the times of discharging and charging with the same current, respectively.

Results and discussion

Characteristic physico-chemical properties of the material

Fig. 1 shows the XRD patterns of rGO/PANI and rGO. From Fig. 1, it is realized that the two rGO/PANI and rGO materials have XRD patterns which are quite similar in shape, with the characteristic peak of graphene at $2\theta \approx 25{,}14$ °. Obviously, bearing rGO onto PANI causes no influence on the structure of graphene.

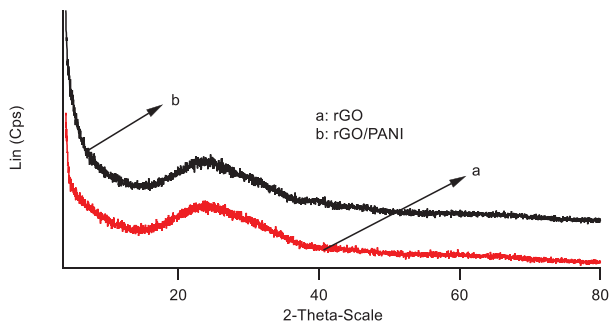

Fig 1. XRD patterns of rGO/PANI and rGO

Fig. 2 shows the TEM images of rGO (a) and rGO/PANI (b). In Fig. 2.b, in addition to graphene sheets as observed in Fig. 2.a, there are also adhesive layers between these graphene sheets. This is thought to be the polymer material in the crystalline structure of rGO/PANI.

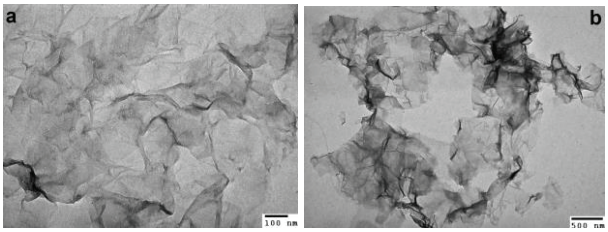

Fig 2. TEM images of rGO (a) and rGO/PANI (b)

The S_{BET} specific surface area measurement (Table 1) indicates that the rGO/PANI material has a much higher specific surface area than the rGO material, which is consistent with Li Tang's argument [13]. Accordingly, thin PANI layers covering the surface and alternating between graphene sheets increase the specific surface area of the material. This nearly double increase in rGO/PANI's specific surface area value over rGO is expected to improve the electrical storage, transmission and discharge properties of the material.

Table 1. S_{BET} value of rGO/PANI and rGO

Sample	The S_{BET} specific surface area (m^2/g)
rGO	257,42
rGO/PANI	578,26

Determining electroactive properties of rGO/PANI

Fig. 3 displays CV measurement result of the rGO/PANI. For ideal capacitors, the CV line is rectangular, highly symmetric because of low contact resistance [14]. For the three-electrode implant system, as in the study of large CV distortion, reduction of symmetry led to narrow loop and oblique angle [15]. At low scanning speed (less than 50 mV s^{-1}), the CV lines obtained are nearly rectanglar as in the case of ideal capacitors, resulting in simplicity and high accuracy in the determination of specific capacitance of rGO/PANI from the CV scan results. The specific capacitance values of rGO/PANI (calculated by formula (1)) reach 82 F g^{-1} and 105 F g^{-1} at scan rate of 5 mV s^{-1} and 50 mV s^{-1}, respectively. When the scan rate increases up to 50 mV s^{-1}, a faraday current is generated against the current direction that the material accumulates and releases in the sweeping current flow measurement, which affects the rate of change. the specific capacitance as well as the reduction in accuracy when determining this value through the circulating current scanning line method. In general, the rGO/PANI's own capacitance increases with increasing scan rate.

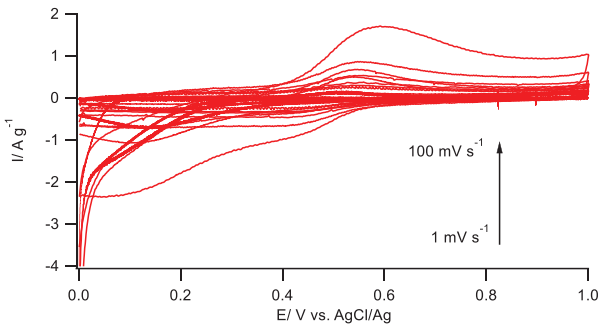

Fig 3. CV curves of rGO/PANI in H_2SO_4 1 M at different scan rates.

The results of the charge-discharge cycle of rGO and rGO/PANI respectively are shown in Fig. 4, 5. From the results obtained, it can be easily to observe that total discharge time (of discharge cycle) is inversely proportional with the increase of the current density. According to formula (2), C_s is proportional to the discharge cycle, so it is inversely proportional to the current density. This is consistent with the results of previously published studies in the world [2-15]. In charge-discharge cycle, with fixed measuring range, the greater the current density is, the greater the amount of charge provided to the material in a unit of time is, which makes it easier to reach the voltage level, and shortens time of energy storage of the material (t_C decreases). It can also be understood that the lower the current density is, the more time required to fill or emit H^+ ions is. With ideal capacitors, at the same constant current density, the charging cycle and the discharging cycle of the capacitor are equivalent, so the smaller t_C is, the smaller t_D is, which reduces C_s.

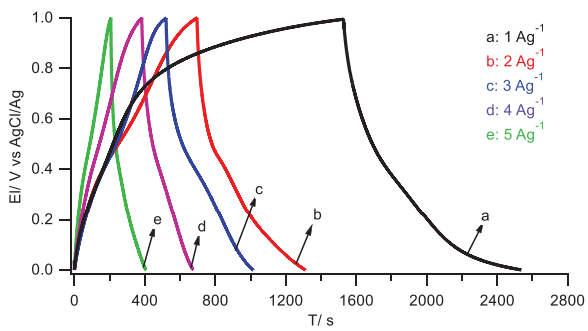

Fig 4. Galvanostatic charge/discharge curvens of rGO/PANI in H_2SO_4 1M at different current densities

Both rGO and rGO/PANI exhibited a very quickly increasing charge-discharge cycle when the current density decreased from 5 A g^{-1} to 1 A g^{-1}. Concurrently, the charge-discharge cycle of rGO/PANI was much higher than that of rGO, which means that the specific capacitance value of rGO/PANI was much greater than that of rGO, at any current density values. The specific capacitance values of the materials at the different current densities are listed in Table 2.

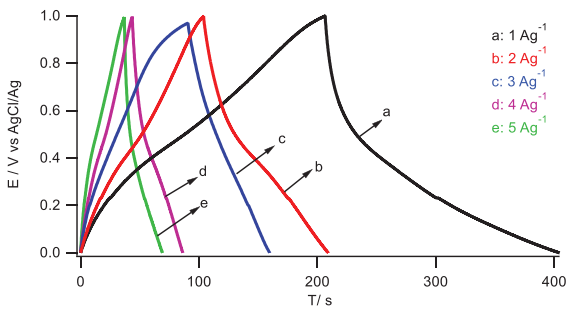

Fig 5. Galvanostatic charge/discharge curvens of rGO in H_2SO_4 1 M at different current densities

Table 2. Specific capacitance of rGO and rGO/PANI at different current densities

I (A g^{-1})	Cs_{rGO} (F g^{-1})	$Cs_{rGO/PANI}$ (F g^{-1})
5	38	185,6
4	42	307,3
3	83	460,5
2	115	589
1	182,7	1121,2

The maximum specific capacitance value of the rGO/PANI is 1121.2 F g^{-1} at the current density of 1 A g^{-1}, and the minimum specific capacitance value is 185.6 F g^{-1} at I = 5 A g^{-1}. These values are five times as high as the specific capacitance values at the responding current densities of rGO. This result is in consistence with previously published results of the conductive graphene-polymer material group known as the highest specific capacitance group up to now [5]. Obviously, the combination of PANI and graphene greatly improves the specific capacitance of material group, which is explained by the increase of surface area, boosting the electrical conductivity as well as improving the diffusion rate of ions during charge-discharge cycle [16]. This combination of PANI and graphene enhances the stability of the rGO/PANI structure during charge-discharge cycle, increasing the specific capacitance as well as the stability of the material [13].

Fig. 6 exhibits the results of the specific capacitance variation and the Coulombic efficiency of rGO and rGO/PANI in terms of current density. The Coulombic efficiency of rGO/PANI at different current density values is higher than that of rGO. This result shows that charge-discharge efficiency of rGO/PANI is better than that of rGO, which means that less electricity is consumed.

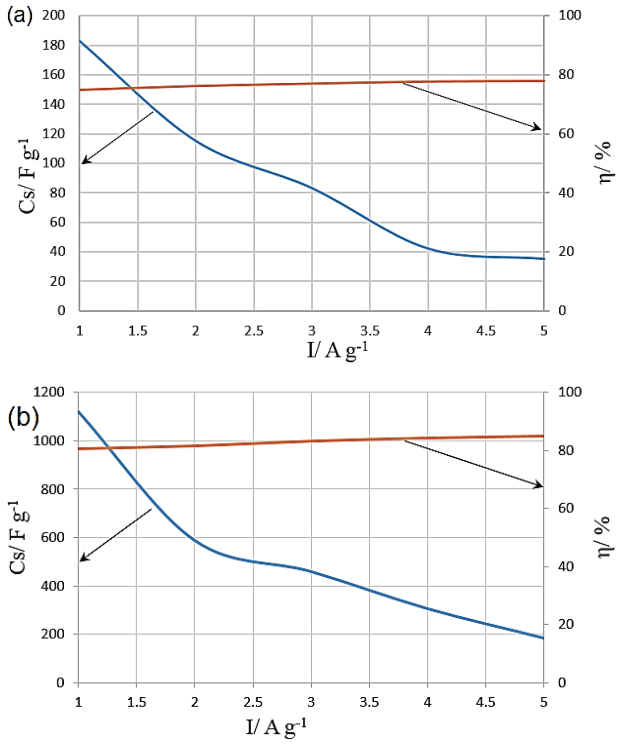

Fig 6. Specific capacitance and Coulombic efficient of rGO (a), rGO/PANI (b) in H_2SO_4 1 M at diffirent current densities.

Electrochemical stabiliti off rGO/PANI

The result of determining the charge-discharge cycle, the specific capacitance variation and the Coulombic efficiency of rGO/PANI and rGO are respectively shown in Fig. 7, 8.

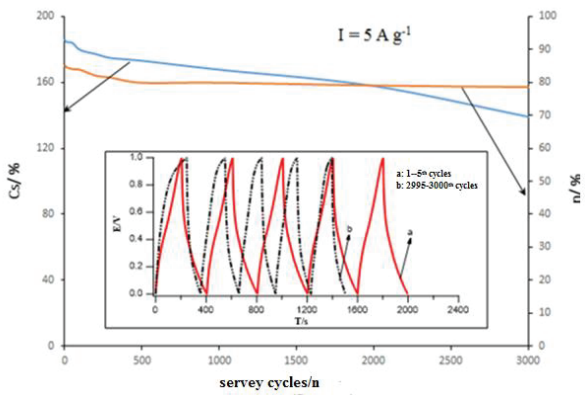

Fig 7. Specific capacitance and Coulombic efficient of rGO/PANI in H_2SO_4 1 M at 5 A g^{-1} befor 3000 cycles charge/discharge curves

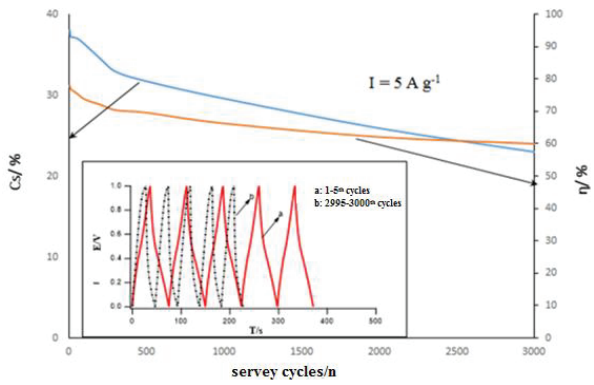

Fig 8. Specific capacitance and Coulombic efficient of rGO in H_2SO_4 1 M at 5 A g^{-1} befor 3000 cycles charge/discharge curves

During 3000 of charge-discharge cycle, rGO/PANI showed the decrease in discharging time as well as its respective specific capacitance value. In early cycles, this decline was slow and unclear. As for rGO/PANI material, the first charge-discharge cycle earned the specific capacitance value of 185.62 F g^{-1}, and at the fifth cycle, the value was 184.69 F g^{-1}, down 0.5 % compared to the former. After 1000 cycles, the specific capacitance of rGO/PANI noticeably reduced as the discharging cycle decreased rapidly, and the charge-discharge cycle ratio became less than 1. At the 1000th cycle, the C_s of rGO/PANI was 167,65 F g^{-1}, down about 10 % compared to the first cycle. The specific capacitance values for this material at the 2000th and 3000th charge-discharge cycle were 157.77 F g^{-1} and 139.22 F g^{-1}, down 15 % and 25 % compared to the first cycle, respectively. At the same time, the rGO material showed a more significant reduce in charge-discharge cycle and specific capacitance values than rGO/PANI. Only after the first 5 charge-discharge cycle, the specific capacitance value of rGO decreased by 1.9 % compared to the original value; The decline at the 1000th, 2000th and 3000th charge-discharge cycle was 22.2 %, 30 % and 37.3 %, respectively, much higher than rGO/PANI.

The results obtained from rGO/PANI are better than those of Hang Sun's publication at the same conditions [6], when the rGO/PANI sample of this author has a 23 % reduction in the specific capacitance immediately after the first 1000 charge-discharge cycle

Conclusions

A nanocomposite rGO/PANI, which can be directly used as electrodes material for a supercapacitor, was successfully prepared. The combination of PANI and graphene was significantly increased the surface area of the material from 257.42 m^2 g^{-1} (for rGO) to 478.26 m^2 g^{-1} (for rGO/PANI).

The specific capacitance of rGO/PANI in 1 M H_2SO_4 solution is five times higher than that of rGO, at all currents density in the charge-discharge cycle measurement. The maximum specific capacitance of rGO/PANI is 1121.2 F g^{-1} compared to 185.5 F g^{-1} of rGO, at 1 A g^{-1}

The electrochemical results also show the high activity stability of rGO/PANI in H_2SO_4 1 M solution with the charge-discharge cycle measurement, Specifically, After 3000 cycles working at 5 A g^{-1}, the specific capacitance retention of rGO/PANI is about 75 % compared to the first cycle, higher than rGO (62.7 %).

The results show that the rGO/PANI material has the potential to be used in coating electrode of supercapacitors.

Acknowledgment

The authors gratefully acknowledge the financial supports from the Ministry of Industry and Trade through the contract number 077.17.ĐT/HĐ-KHCN.

References

1. Chenguang Liu, Zhenning Yu, David Neff, Aruna Zhamu, and Bor Z. Jang, Graphene-Based Supercapacitor with an Ultrahigh Energy Density, Nano Letters, (2010) 10 (12) 4863–4868.
2. Bing Zhao, Peng Liua, Yong Jiang Dengyu Pan, Haihua Tao, Jinsong Song, Tao Fang, Weiwen Xu, Supercapacitor performances of thermally reduced graphene oxide, Journal of Power Sources (2012) 198, 423–427.
3. Sheng Zhu, Mi Wu, Mei-Hong Ge, Hui Zhang, Shi-Kuo Li, Chuan-Hao Li, Design and construction of three-dimensional CuO/polyaniline/rGO ternary hierarchical architectures for high performance supercapacitors, Journal of Power Sources 306 (2016) 593-601.

4. Van Hoa Nguyen and Jae-Jin Shim, Ultrasmall SnO_2 nanoparticle-intercalated graphene -@polyaniline composites as an active electrode material for supercapacitors in different electrolytes, Synthetic Metals 207 (2015) 110–115.
5. Fuyou Ke, Yu Liua, Hongyao Xu, Yu Maa, Shanyi Guang, Fayin Zhang, Naibo Lin, Meidan Ye, Youhui Lin, and Xiangyang Liu, Flower-like Polyaniline/Graphene Hybrids for High-Performance Supercapacitor, Composites Science and Technology, 142 (2017) 286-293.
6. Hang Sun, Ping She, Kongliang Xu, Yinxing Shang, Shengyan Yin, Zhenning Liu, A self-standing nanocomposite foam of polyaniline@reduced graphene oxide for flexible super-capacitors, Synthetic Metals 209 (2015) 68–73.
7. Jun Yao, Qingjiang Pan, Shanshan Yao, Limei Duan and Jinghai Liu, Mesoporous MnO_2 Nanosphere/Graphene Sheets as Electrodes for Supercapacitor Synthesized by a Simple and Inexpensive Reflux Reaction, Electrochimica Acta, 238 (2017) 30-35.
8. Nidhi Agnihotri, Pintu Sen, Amitabha De and Manabendra Mukherjee, Hierarchically designed PEDOT encapsulated graphene-MnO_2 nanocomposite as supercapacitors, Materials Research Bulletin 88 (2017) 218–225.
9. Pengfei Wang, Hui Liua, Yuxing Xu, Yunfa Chen, Jun Yang, Qiangqiang Tan, Supported ultrafine ruthenium oxides with specific capacitance up to 1099 F/g for a supercapacitor, Electrochimica Acta, 194, 211-218, 2016.
10. Sangeun Cho, Jongmin Kim, Yongcheol Jo, Abu Talha Aqueel Ahmed, H.S.Chavan, Hyeonseok Woo, A.I. Inamdar, J.L. Gunjakar, S.M. Pawar, Youngsin Park, Hyungsang Kim and Hyunsik Im, Bendable RuO_2/graphene thin film for fully flexible supercapacitor electrodes with superior stability, Journal of Alloys and Compounds 725 (2017) 108-114.
11. Thu Ha Thi Vu, Thanh Thuy Thi Tran, Hong Ngan Thi Le, Lien Thi Tran, Phuong Hoa Thi Nguyen, Nadine Essayem; Pt-AlOOH-SiO_2/graphen hybrid nanomaterial with very high electrocatalytic performance for methanol oxidation, Journal of Power Sources 276 (2015) 340-346.
12. Wenjuan Wang, Qingli Hao, Wu Lei, Xifeng Xia, Xin Wang, Ternary nitrogen-doped graphene/nickel ferrite/polyaniline nanocomposites for hing-performance supercapaitors, Journal of Power Sources 269 (2014), 250-259.
13. Li Tang, Zhaokun Yang, Fang Duan, Mingqing Chen, Fabrication of graphene sheets/polyaniline nanofibers composite for enhanced supercapacitor properties, Colloids and Suface A: Physicochemical and Engineering Aspects 520 (2017), 184-192.
14. Van Chinh Tran, Van Hoa Nguyen, Thi Toan Nguyen, Jae Heung Lee, Dang Chinh Huynh, Jae-Jin Shim, Polyaniline and multi-walled carbon nanotube-intercalated graphene aerogel and its electrochemical properties, Synthetic Metals 215 (2016), 150-157
15. Guangqiang Han, Yun Liu, Lingling Zhang, Erjun Kan, Shaopeng Zzhang, Jian Tang, Weihua Tang, MnO_2 nanoroads intercalating Graphene oxide/polyaniline ternary composites for robust high-performance supercapacitors, Scientific Reports 4 (2018), 1-7.
16. Zhe-Fei Li, Hangyu Zhang, Qi Liu, Lili Sun, Lia A. Stanciu and Jian Xie, Fabrication of high-surface-area graphene/polyaniline nanocompostes and their application in supercapacitors, Applied Materials & Interfaces, 5 (7) (2013), 2685-2691.